Biosensors and Bioelectronics 81 (2016) 68–74

Contents lists available at ScienceDirect

Biosensors and Bioelectronics

journal homepage: www.elsevier.com/locate/bios

Choline-induced selective fluorescence quenching of acetylcholinesterase conjugated Au@BSA clusters

Meegle S. Mathew [a], Ananya Baksi [b], T. Pradeep [b], Kuruvilla Joseph [a,*]

[a] Department of Chemistry, Indian Institute of Space Science and Technology, Valiyamala, Thiruvananthapuram 695547, India
[b] DST Unit of Nanoscience (DST UNS), and Thematic Unit of Excellence (TUE), Department of Chemistry, Indian Institute of Technology Madras, Chennai 600036, India

ARTICLE INFO

Article history:
Received 24 November 2015
Received in revised form
9 February 2016
Accepted 16 February 2016
Available online 20 February 2016

Keywords:
Acetylcholinesterase (AChE)
Acetylcholine (ACh)
Choline
Quantum Clusters
Fluorescence
Quenching

ABSTRACT

We have developed a highly selective sensitive fluorescent detection of acetylcholine (ACh) using bovine serum albumin (BSA) protected atomically precise clusters of gold. The gold quantum clusters (Au_{QC}@BSA) synthesized using bovine serum albumin and conjugated with acetylcholinesterase (AChE), an enzyme specific for acetylcholine, resulting in Au_{QC}@BSA-AChE. The enzyme, AChE hydrolyzes acetylcholine (ACh) to choline (Ch) which in turn interacts with Au_{QC}@BSA-AChE and quenches its fluorescence, enabling sensing. We have carried out the real time monitoring of the hydrolysis of ACh using electrospray ionization mass spectrometry (ESI MS) to find out the mechanism of fluorescent quenching. The validity of present method for determination of concentration of acetylcholine in real system such as blood was demonstrated. Further, the sensor, Au_{QC}@BSA-AChE can be easily coated on paper and an efficient and cheap sensor can be developed and detection limit for ACh is found to be 10 nM. The fluorescent intensity of Au_{QC}@BSA-AChE is sensitive towards acetylcholine in range of 10 nM to 6.4 μM. This suggests that Au_{QC}@BSA-AChE has an excellent potential to be used for diagnosis of various neuropsychological and neuropsychiatric disorders.

1. Introduction

Noble metal quantum clusters are one of the fascinating research areas due to their exciting photophysical and chemical properties. An attractive property of these clusters is their luminescence in the visible and near infrared regions (Huang and Murray, 2001). Besides monolayer protection, macromolecular template-based cluster synthesis is also drawing great attention due to the high bio-compatibility and intense luminescence of the resulting clusters (Feng et al., 2013; Le Guèl vel et al., 2011; Li et al., 2012, 2013). Their easy one-step and green synthesis makes them particularly attractive (Lin et al., 2009; Liu et al., 2013; Xie et al. 2009). Several proteins have been used for such cluster synthesis among which bovine serum albumin (BSA) based system has been the most widely studied (Baksi et al., 2013b; Das et al., 2012; Liu et al., 2013; Lystvet et al., 2013; Raut et al., 2013a, 2013b). However, these clusters have not been crystallized so far, unlike their monolayer protected analogs (Bellon et al., 1972; Heaven et al., 2008). They are mostly characterized by mass spectrometry (MS) and specifically by matrix assisted laser desorption ionization (MALDI) MS to get an idea about the cluster core (Baksi et al., 2013a; Dass, 2009).The intense red luminescence exhibited by the protein protected clusters is being increasingly explored in the development of fluorescence based sensors (Chen et al., 2014; Mathew and Pradeep, 2014; Shang et al., 2011; Zhang et al., 2013).

Acetylcholine (ACh) is one of the most important neurotransmitters found in the human central and peripheral nervous systems. Acetylcholinesterase (AChE) catalyzes the hydrolysis of ACh to choline and acetate (Soreq and Seidman, 2001). It is mainly found at the neuromuscular junction and in animal synapse. Its main function is to terminate the signaling triggered by ACh release (He et al., 2014). An abnormally low concentration of ACh can cause various neuropsychological and neuropsychiatric disorders such as Alzheimer's disease, Parkinson's disease (Blokland, 1995) etc. The main reason behind the Alzheimer's disease is the decreased levels of ACh and the enzymes responsible for its synthesis and degradation in the brain (Mueller et al., 2005). Thus, by monitoring the activity of AChE and measuring the concentration of ACh in the human body, one could detect Alzheimer's in its early stage. The level of ACh of a healthy person in blood can be varied from 0.20 to 1.31 μM/liter with a geometric mean of 0.49 μM /liter (Watanabe et al., 1986). Clearly, a patient suffering from Alzheimer's will have still lower level of ACh than 0.20 μM

* Corresponding author.
E-mail addresses: Pradeep@iitm.ac.in (T. Pradeep), kjoseph.iist@gmail.com, kuruvilla@iist.ac.in (K. Joseph).

http://dx.doi.org/10.1016/j.bios.2016.02.048
0956-5663/

ACh (Mueller et al., 2005; Watanabe et al., 1986). Thus, our sensor (AuQC@BSA-AChE) can be used for early stage diagnosis of neuropsychiatric diseases such as Alzheimer's, Parkinson's etc.

Recently, Wei and co-workers have detected ACh using carbon dots (Wei et al., 2014). They have developed a biosensor for the detection of acetylcholine based on the detection of H_2O_2. In this process, ACh decomposes into choline and acetate by AChE. The product choline is decomposed further by another enzyme, choline oxidase (ChOx) to betaine and H_2O_2, followed by Fenton reaction and the resulting hydroxyl group quenches fluorescence of carbon dot. Johnson et al. designed a semi-synthetic fluorescence-based probe, ACh-SNIFIT, for direct, real-time detection of acetylcholine and anticholinesterase (Schena and Johnsson, 2014). Liu and co-workers utilized Rhodamine B modified gold nanoparticles for sensing AChE (Liu et al., 2012). The above mentioned sensors are based on the principle of fluorescence quenching or enhancement and typically employ organic dyes. However, many of organic fluorophores are toxic and unstable with a poor selectivity for the target analyte and hence practical applications for real systems are difficult to achieve. In comparison, protein protected clusters are bio-compatible and can be used as effective probes for sensing (Xavier et al., 2012). Recently Chen and his co-workers developed a sensor for detection of activity of Acetylcholinesterse enzyme using denatured BSA protected cluster. They have indirectly detected activity of acetylcholinesterase using acetylthiocholine iodide as substrate (Li et al., 2014). Here, we report a novel bio-friendly fluorescence based direct detection of ACh using AChE conjugated BSA protected gold quantum clusters (QCs), (Au_{QC}@BSA-AChE). We have developed a highly selective and sensitive detection of ACh via its hydrolysis to choline and acetate by AChE. The generated choline interacts with the Au QCs and quenches the latter's fluorescence. The practicality of the Au_{QC}@BSA-AChE sensing system was validated through the detection of ACh in blood samples. The Au_{QC}@BSA-AChE can be easily coated on a filter paper and an efficient sensor with a low detection limit of 0.01 μM can be constructed.

2. Material and methods

2.1. Materials

All the reagents were used as obtained without further purification unless stated otherwise. $HAuCl_4.3H_2O$, BSA, the membrane dialysis bag (molecular weight cut-off 12 kDa), AChE (Type C3389, 500 U mg^{-1} from electric eel), acetylcholine chloride, choline chloride, glucose, fructose, glycine, lysine, sodium dihydrogen phosphate, and disodium hydrogen phosphate were purchased from Sigma Aldrich. All solutions were prepared using Millipore water. Stock solutions of ACh, choline and AChE were prepared using phosphate buffer of pH 8 (0.05 M).

2.2. Detection of acetylcholine in blood

Blood samples were collected from a healthy adult volunteer and samples were spiked with different concentration of acetylcholine and incubated for 30 min. The above ACh spiked blood and blood without ACh spike is treated with 3 mL of Au_{QC}@BSA-AChE and changes in fluorescent intensity at 670 nm was monitored. This study was approved by ethical committee of Indian Institute of Space Science and Technology (IIST) (IIST/IEC/2016/CHE-01).

2.3. Instrumentation

UV–visible absorption spectra were recorded in the range of 200–800 nm using the Varian model, Cary win Bio 100 spectrometer. All fluorescence measurements were made using the Fluoro Max-4C spectrofluorometer (Horiba Instruments, USA). The emission spectra were recorded upon excitation at 365 nm; the slits for excitation and emission were set at 5 nm. High resolution transmission electron microscopy (HRTEM) images were obtained with a JEOL 3010 instrument. For MALDI TOF MS analysis, the Applied Biosystems Voyeger-DE-pro instrument was used and sinapic acid was used as the matrix. Particle size and zeta potential measurements were performed using particle size analyzer (ZetasizerNano ZS series, Malvern instruments). High pressure liquid chromatography analysis was carried out using shimadzu high pressure liquid chromatography, Japan.

Electrospray ionization (ESI) MS studies were conducted in the mass range of m/z 80 to 1700 using the Applied Biosystems 3200 QTRAP LC/MS/MS system. The following optimized conditions were used: declustering potential (DP)=30 V, entrance potential (EP)=10 V, ion spray voltage (ISV)=2.5 kV, and flow rate=3 μL/min.

2.4. Synthesis

2.4.1. Synthesis of Au_{QC}@BSA

The red luminescent Au_{QC}@BSA was synthesized by a previously reported method (Mohanty et al., 2015). Briefly, 10 mL aqueous solution of $HAuCl_4$ (6 mM) was added to 10 mL BSA (25 mg/mL in water) with vigorous stirring for 5 min, followed by the addition of 1 mL of 1 M NaOH solution to maintain the basicity (pH 12) of the system. The reaction was continued for 24 h under mild stirring. The golden yellow solution slowly changed to dark orange with intense red luminescence under UV irradiation, indicating the formation of gold QCs. Purification of Au_{QC}@BSA was performed by dialysis against distilled water for 24 h in a dialysis membrane of molecular weight cut-off 12 kDa. The cleaned gold clusters were then freeze dried and stored at 4 °C for further use.

2.4.2. Synthesis of Au_{QC}@BSA-AChE

Synthesis of Au_{QC}@BSA-AChE was carried out by mixing of AChE with Au_{QC}@BSA. The dialysed and freeze dried gold clusters were dissolved in a phosphate buffer at pH 8, since the optimum pH for AChE activity is 8-9. Au_{QC}@BSA-AChE was prepared by treating 10 mL of the gold cluster solution with 1 mL of AChE (0.4 μM) dissolved in phosphate buffer (pH 8) at room temperature under mild stirring, followed by a reaction time of 2 h and stored at 4 °C for further use.

2.4.3. Development of test strips for detection of ACh

The Au_{QC}@BSA-AChE coated sensor was developed in a simple way. Briefly, Whatman No 41 filter paper were cut into small pieces (2 cm × 2 cm) and soaked in 10 mL Au_{QC}@BSA-AChE (at a concentration of 0.4 μM) solution taken in a beaker for about 24 h. After drying in air (approximately 2 hour), 20 μL of different concentration of ACh is drop casted. The Au_{QC}@BSA-AChE coated sensor before and after the treatment of ACh is placed under UV light (360 nm) and changes in the color has been noted.

3. Results and discussion

3.1. Designing the Au_{QC}@BSA-AChE conjugate

A schematic of our experiment is shown in Scheme 1. We have synthesized highly fluorescent BSA protected gold quantum clusters (Au_{QC}@BSA). MALDI MS showed the presence of Au core containing 30 atoms with a molecular ion peak at m/z 72 kDa, based on which the cluster was assigned as Au_{30}@BSA. Parent BSA

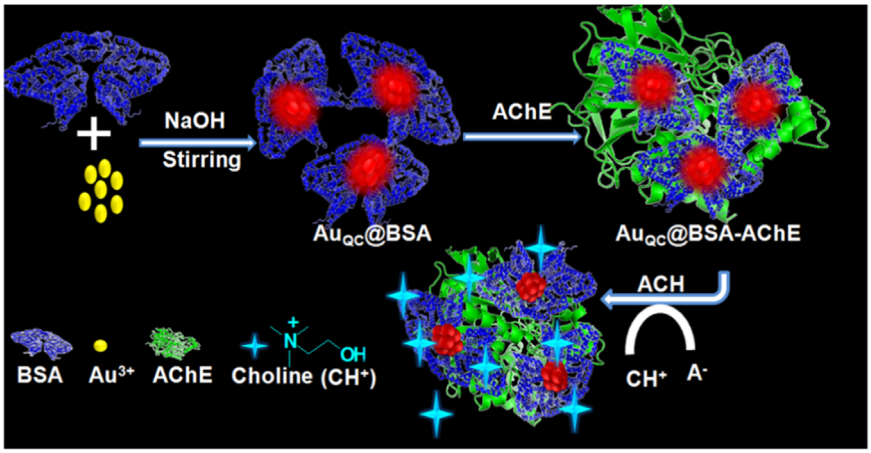

Scheme 1. Schematic representation of synthesis of Au_{QC}@BSA, Au_{QC}@BSA-AChE and consecutive detection of acetylcholine via fluorescence quenching.

exhibits a mass peak at *m*/*z* 66 kDa (Fig. S1(a), supplementary material). Presence of larger plasmonic nanoparticles in the sample was ruled out by UV–vis absorption spectra (absence of plasmon band at 520 nm) and transmission electron microscopy (TEM) (size of the particles seen was of about 1 nm) (Fig. S1(b), supplementary material). The cluster solution shows a red luminescence under UV exposure. The emission maximum is at 677 nm with an excitation maximum at 365 nm (Fig. S1(d))

Recently, Mohanty et al. have shown that BSA can form conjugate with lysozyme (Lyz) by simple mixing with each other (Mohanty et al., 2015). Proteins are well known to form aggregates mostly due to salt bridge interaction between one unit with the other. Mixed protein conjugates are also possible when multiple proteins are present in the same mixture. Lakshmi et al. also reported that conjugation of glutathione protected Au cluster and urease can be accomplished by mixing Au cluster and urease (Nair et al., 2013). We have carried out conjugation of AChE over Au_{QC}@BSA by mixing AChE with Au_{QC}@BSA and stirred for 2 h. There was no considerable change in the optical properties of cluster before and after the treatment of AChE. UV–Visible and PL spectra of Au_{QC}@BSA before and after the addition of ACh are shown in Fig. S2 of supplementary material. Due to the instrumental limitation, number of AChE conjugated to the cluster were unable to found out because of the large mass of AChE (260 kDa for AChE whereas mass of the Au_{QC}@BSA is around 72 kDa). Transmission electron microscopy image shows that size and morphology of the cluster remains same after conjugation of AChE (Fig. S2). Further we have analyzed the change in hydrodynamic volume of Au_{QC}@BSA before and after conjugation of enzyme using dynamic light scattering technique. Here after conjugation of AChE, average diameter of Au_{QC}@BSA is changed from 10.29 nm to 18.17 nm, which implies the adsorption of AChE over AuQC@BSA (Fig. S2). Zeta potential measurements were performed before and after the treatment of AChE. The studies showed a significant decrease in zeta potential of Au_{QC}@BSA from −20 mV to −12 mV after AChE treatment. This reflects the conjugation AChE to Au_{QC}@BSA through strong electrostatic interaction between Au_{QC}@BSA and AChE.

3.2. Sensing of acetylcholine

The fluorescence emission intensity of Au_{QC}@BSA-AChE was readily quenched in the presence of ACh. Scheme. S1 of supplementary material shows the hydrolysis of ACh to choline and acetate in presence of AChE. Fig. 1a illustrates the decrease in fluorescence of Au_{QC}@BSA-AChE as a function of increasing concentration of ACh. Specifically, on addition of 6.4 μM ACh, nearly 60% of the fluorescence emission intensity of Au_{QC}@BSA-AChE was quenched. A Linear correlation between the two quantities, i.e. emission intensity and concentration, is clearly visible from the Stern–Volmer plot, displayed in Fig. 1b. The plot is constructed based on the Stern–Volmer equation, $F_0/F = 1 + K_{SV}[Q]$, where the F_0 and F represent the fluorescence intensity of Au_{QC}@BSA-AChE in the absence and the presence of ACh respectively, K_{SV} is the Stern–

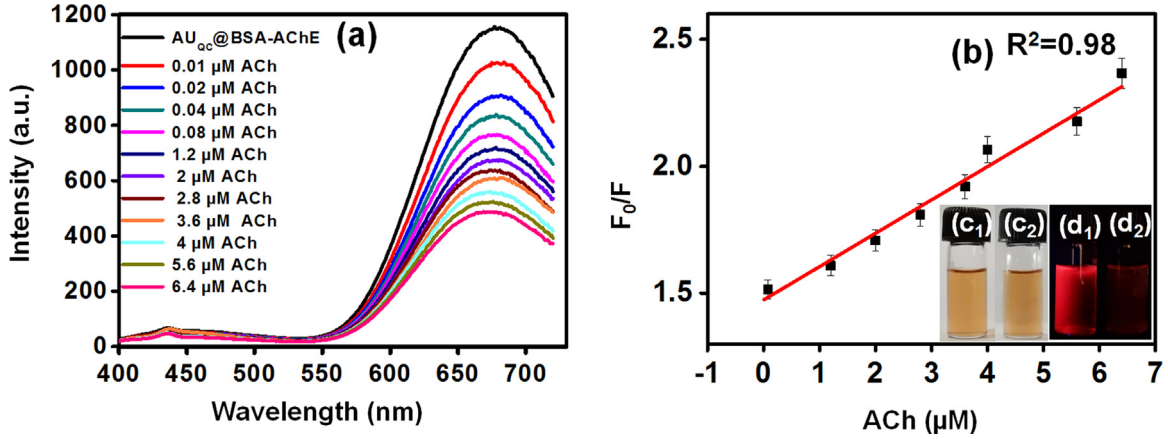

Fig. 1. (a) Variation of the fluorescence emission spectrum of Au_{QC}@BSA-AChE with increasing concentration of ACh is showing continuous decrease in emission intensity with increase in ACh concentration. (b) The Stern–Volmer plot depicting the linear correlation between fluorescence emission intensity at 677 nm and ACh concentration. c_1 and c_2 are the photograph of Au_{QC}@BSA-AChE before and after treatment with ACh (6.4 μM) in visible light and d_1 and d_2 in UV light respectively.

Volmer quenching constant, and [Q] is the concentration of analyte. The figure shows that Au_{QC}@BSA-AChE is highly sensitive to ACh concentrations within the dynamic range of 0.08 μM to 6.4 μM with $R^2=0.98$.The Stern volmer plot is constructed using a subset of data points taken from Fig. 1A and the complete plot is given as Fig. S3 of supplementary materials. Inset of Fig. S3 shows the linearity in the lower concentration of ACh (0–0.04 μM). It is observed from the Fig. 1a that rate of quenching is more at lower concentration of ACh (0–0.04 μM) compared to higher concentration. The quenching of fluorescence is also easily noticeable from the photographs (insets in Fig. 1b) of Au_{QC}@BSA-AChE solution before and after treatment with ACh (6.4 μM). Detailed mechanism of the fluorescence quenching of Au_{QC}@BSA-AChE by ACh is given in Section 3.5.

3.3. Selectivity studies

We have investigated the selectivity for detection of ACh by comparing the fluorescence response of Au_{QC}@BSA-AChE to the presence of other biologically relevant molecules and neurotransmitter (dopamine) under similar reaction conditions. We have tested several molecules and salts (ions derived from them), namely, glucose (Glu), fructose (Fruct), lactose (Lact), glycine (Gly), lysine (Lys), cysteine (Cys), homocysteine(Hcys), glutathione (GSH) NaCl and KCl, which are normally present in blood and could therefore be responsible for fluorescence quenching in a real system. We found that amongst these, only ACh led to significant decrease of fluorescence intensity of Au_{QC}@BSA-AChE, while other molecules did not affect it much as shown in Fig. 2a. Furthermore another neurotransmitter, dopamine slightly enhanced the fluorescence intensity when 6.4 μM concentration of dopamine is introduced as can be seen in Fig. 2a. On the contrary, no variation in the fluorescence signal of Au_{QC}@BSA-AChE is observed when the concentration of dopamine is <6.4 μM. This clearly indicates that, dopamine is less likely to interfere in the acetylcholine detection in real systems, as its concentration is much below 6.4 μM (Zhang et al., 2003). Further, we extended our selectivity studies to co-existing system, performed in two ways. Firstly, the fluorescence spectra of the mixture of ACh and each of the above analytes were recorded and secondly, the fluorescence studies of the mixture of ACh and all the above analytes were performed. Concentration of ACh and the analytes were maintained at 6.4 μM and the corresponding plot showing the variation in fluorescence intensity verses the various co-existing mixture is shown in Fig. S4, supplementary material. Obviously, in all these cases the change in fluorescence intensity of Au_{QC}@BSA-AChE is nearly equal to the extent of quenching of Au_{QC}@BSA-AChE by ACh alone, which reflects the negligible interference from the above mentioned analytes when they are present in mixture. Detection limit of the present sensor towards ACh is 10 nM, a noticeable quenching in the fluorescence intensity of Au_{QC}@BSA-AChE is found at this concentration (Fig. 2b).

We have compared the analytical performance of the current method with various other analytical tools used for ACh detection in recent times (Table S1, supplementary material). It is clear from the table that, the analytical parameters such as detection limit, dynamic range of the present sensor is comparable/superior to the many of the mentioned methods.

3.4. Kinetics of interaction of acetylcholine with Au_{QC}@BSA-AChE

To understand the kinetics of fluorescence quenching, the ESI MS spectra of the enzymatic reaction was monitored over real time. The decrease in signal intensity of acetylcholine and a gradual increase in choline intensity with increasing time of reaction was observed (Fig. 3a). Under the optimized conditions, at pH 8 the conversion of ACh (0.4 μM AChE) to choline was completed within 1 h. In comparison, when Au_{QC}@BSA-AChE was used at pH 8 (at a concentration of 0.4 μM), ACh was consumed and transformed to choline in ≈ 5 min (see Fig. 3b). Thus, it is evident from the time variation of ESI MS that rapid detection of acetylcholine is possible by using the Au_{QC}@BSA-AChE conjugate system.

3.5. Mechanism of fluorescence quenching

The high concentration of choline that is produced rapidly near the enzyme as confirmed by the above MS investigation could interact with the cluster system and can lead to fluorescence quenching. To confirm this, we performed control experiments in which similar concentrations of choline were allowed to interact with the Au_{QC}@BSA-AChE cluster and found that choline effectively quenches the fluorescence intensity (Fig. S5(b), supplementary material). Note that choline consists of an electron deficient quaternary ammonium group and an alkyl hydroxyl group, either of which can interact with the cluster. To identify the underlying mechanism, we examined the interaction between Au_{QC}@BSA-AChE and different molecules containing these two functional groups individually. We mimicked the quaternary ammonium group using quaternary ammonium bromide and found that these compounds are efficient quenchers of Au_{QC}@BSA-AChE (Fig. S6), while alkyl alcohols do not show such activity (MeOH, EtOH, etc.) (Fig. S7), hence we confirmed that interaction is mostly

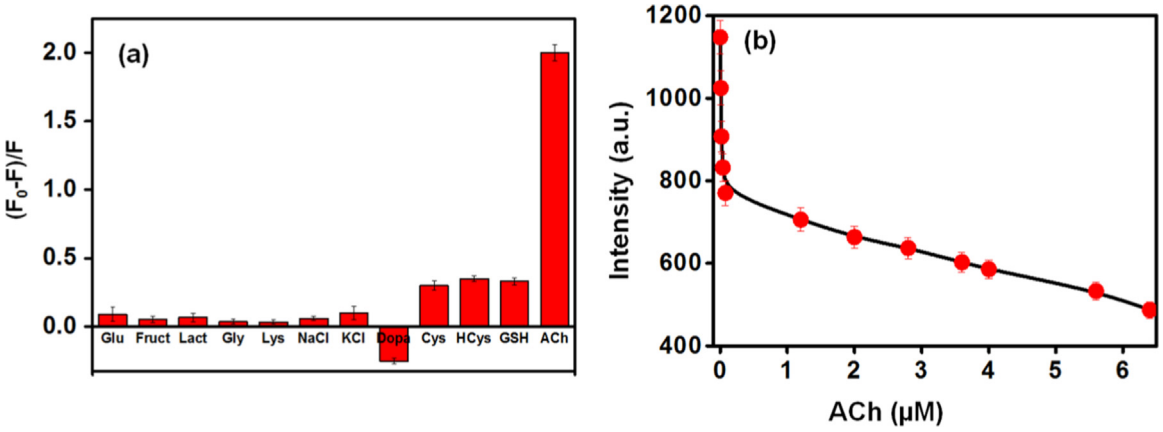

Fig. 2. Effect of various biologically relevant molecules and dopamine, a neurotransmittter on the luminescence intensity of Au_{QC}@BSA-AChE (concentration of all analytes were kept at 6.4 μM). (b) is showing the variation of fluorescence intensity with different concentrations of ACh. Lowest detection limit was found to be 10 nM. The error bar represent standard deviations based on three independent measurements.

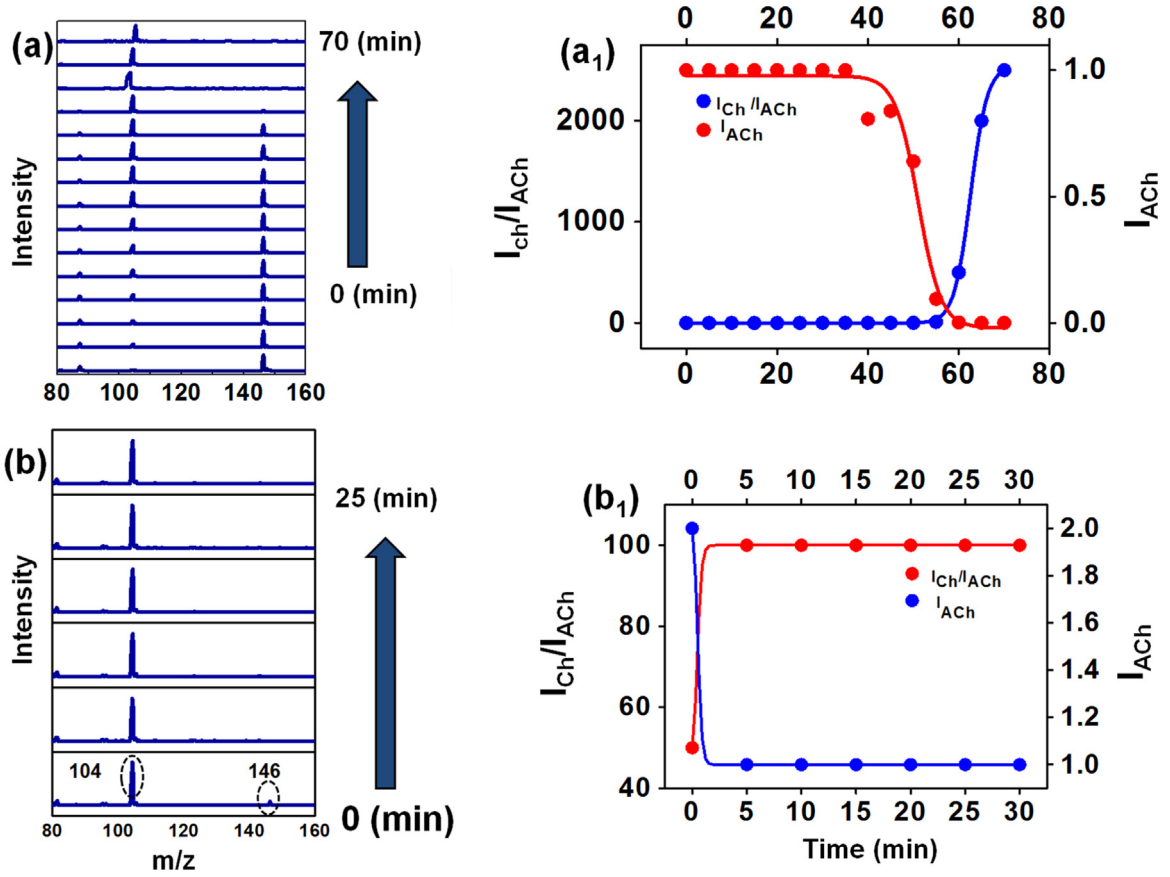

Fig. 3. Real time monitoring of ESI MS of hydrolysis of (a) ACh by AChE over a reaction time of 0–70 min and (b) ACh by Au_{QC}@BSA-AChE over a shorter reaction time of 0–25 min. (a_1) and (b_1) are the corresponding calibration plots depicting the continuous decrease in acetylcholine intensity and a simultaneous increase in choline intensity.

through quaternary ammonium group. Further, interaction of acetate group towards cluster was ruled out by fluorescence study. There is no substantial variation in fluorescence intensity of gold cluster after the treatment of different concentration of acetic acid (Fig. S8).

To support the proposed mechanism, Au@BSA alone was treated with ACh. As displayed in Fig. S5, in comparison with Au_{QC}@BSA-AChE (Fig. S5(a), repeat of Fig. 1a), the fluorescence intensity of Au_{QC}@BSA did not vary significantly even on addition of a high concentration of ACh (10–14 μM) (Fig. S5(c)). This suggests that in the absence of AChE, Au_{QC}@BSA alone cannot hydrolyze acetylcholine to choline. Hence, the observed fluorescence quenching of Au_{QC}@BSA-AChE can only be related to the choline generated through the hydrolysis of ACh by the binding of AChE to the cluster.

The actual mechanism of sensitive response of Au_{QC}@BSA-AChE towards acetylcholine has been investigated. It is well reported that, the stern-volmer plot will give an idea about the fluorescence quenching mechanism (Lakowicz, 2013). Here the linear stern-volmer plot depicts that only one type of quenching takes place, which may be either static or dynamic quenching. To further understand the actual mechanism for fluorescent quenching, we have carried out a detailed study in this system. It is noticed that the fluorescence quenching is not due to the fluorescence resonance energy transfer (FRET) since there is no overlapping between absorption spectrum of acetylcholine and emission spectra of Au_{QC}@BSA-AChE. Another possible mechanism for fluorescence quenching is analyte induced nano aggregation. The analyte induced aggregation may not be possible since gold quantum clusters are stabilized by bovine serum albumine mainly by covalent interaction between gold nanoclusters and the thiol groups of the cysteine. Here choline is not able to substitute BSA and induce aggregation of clusters. Moreover, we did not observe any aggregation even for a long time after addition of ACh to Au_{QC}@BSA-AChE (Fig. S9(a)). It is well reported that interaction analyte towards surface of protein protected cluster can alter its fluorescent intensity (Chen et al., 2012; Hemmateenejad et al., 2014). The probable reason for quenching effect of acetylcholine could be attributed to hydrolysis of acetylcholine and the electrostatic interaction between positively charged choline and negatively charged Au_{QC}@BSA-AChE. Consequently changes the environment of the Au_{QC}@BSA-AChE leads to the static fluorescence quenching of the cluster. It is confirmed from absorption spectrum of Au_{QC}@BSA-AChE before and after addition of acetylcholine (Fig. S9 (b)). There is decrease in absorbance of Au_{QC}@BSA-AChE after each addition of acetylcholine.

3.6. Analysis of ACh in blood samples

To check the validity of the present fluorescent sensor towards the detection of ACh in real system, pre-treated blood samples were spiked with known amount of ACh and fluorescence analysis were performed. Details on sample preparation are included in the experimental section. The blood samples were diluted to 1000-fold prior to analyzing of ACh to avoid interference from matrix. Au_{QC}@BSA-AChE is treated with 50 μL of diluted blood, there is a decrease in fluorescent intensity and further the addition of blood to the same system does not changing fluorescent intensity of cluster. It is confirmed that decrease in fluorescent intensity is due to the presence of ACh in blood (Fig. S10). This suggests that other thiol like group present in the blood had no interference for detection of acetylcholine in blood. Further an apparent decrease in

Table 1
Comparative study of detection of ACh in real sample with the present method.

Test No	Standard addition in blood (μM)	Amount Found (μM)			
		HPLC	RSD (%) ($n=3$)	Our method	RSD (%) ($n=3$)
1	0	0.72	2	0.8	1.7
2	1.2	1.90 (98%)	1.5	1.97 (98.5%)	1.2
3	2.0	2.66 (97%)	1.8	2.75 (98.21%)	1.35
4	2.8	3.55 (100%)	1.4	3.4 (95%)	2

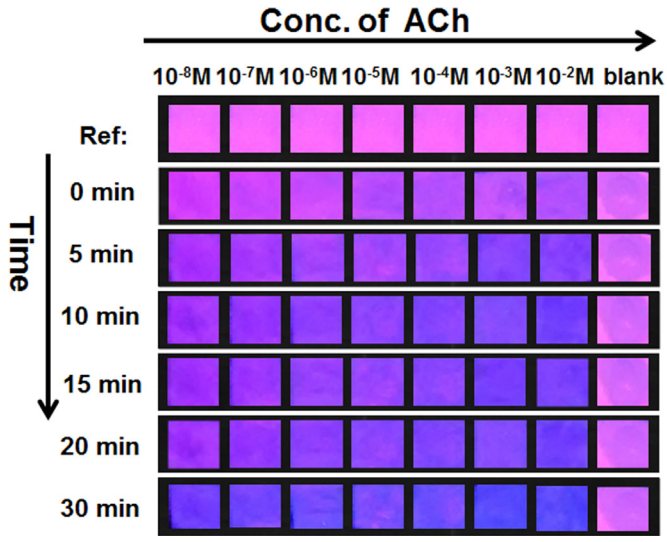

Fig. 4. Shows photographs of the Au_{QC}@BSA-AChE test paper strips with different concentrations of acetylcholine taken under UV light at several time intervals.

fluorescence at 677 nm of the Au_{QC}@BSA-AChE was observed after the treatment of ACh spiked blood samples (Fig. S10). The mean recoveries for ACh at three spiked levels (1.2, 2 and 2.8 μm) ranged from 95 to 98% and the fluorescence responses against the concentrations of ACh spiked into whole blood was linear. Further, to understand accuracy of the present method, we have performed HPLC, a standard method used for detection of ACh in blood sample and ACh spiked blood sample under similar reaction condition. The result depicts that values obtained by present method is in close agreement with one obtained using HPLC analysis (Table 1). These results suggest that this probe is largely free from the matrix effect of the blood sample and accuracy and reliability of the present method for ACh determination in real samples. The concentration of acetyl choline in normal blood was determined to be 0.8 μM using our method and 0.72 μM by using HPLC.

3.7. Sensor development

From the previous studies, we know that Au_{QC}@BSA is stable in the presence of various polymeric supports like fibers. Recently, single fiber based detection of Hg^{2+} (Ghosh et al., 2014) and TNT (Mathew et al., 2012) have been reported, confirming the stability of such clusters on polymeric matrices also. With this motivation, we proceeded to develop a paper based sensor for the visual detection of acetylcholine using Au_{QC}@BSA-AChE. To achieve this, we soaked small pieces of filter paper in Au_{QC}@BSA-AChE overnight and then dried them. We found that over a few months Au_{QC}@BSA-AChE was stable on a filter paper and maintained its emission intensity. Using the Au_{QC}@BSA-AChE test paper, we were able to detect different concentrations of acetylcholine. As the reaction time progressed from 0 to 30 min, color of the paper changed from red to blue under UV the light (Fig. 4). As can be seen from Fig. 4, the emission color is depended on the concentration of ACh. From the time-dependent photographs of the test paper strips in the figure, it is evident that complete quenching occurs within 30 min. We believe that extending the stability of the luminescence on the filter paper would make Au_{QC}@BSA-AChE test strips useful for practical applications.

4. Conclusions

In the present study, we have effectively conjugated the enzyme, acetylcholinesterase (AChE) with BSA protected gold quantum clusters (Au_{QC}@BSA) and used the conjugate for the selective detection of acetylcholine (ACh). The conjugate, Au_{QC}@BSA-AChE exhibits optical properties similar to Au_{QC}@BSA. During the detection of ACh, AChE bound to the Au_{QC}@BSA hydrolyzes ACh to choline, which in turn quenches fluorescence of Au_{QC}@BSA-AChE through the interaction of choline to the gold quantum clusters. A detection limit of ACh of 10 nM is achieved by this method which is far lower than the methods reported so far. Real time monitoring of the hydrolysis via ESI MS shows that the reaction is faster with Au_{QC}@BSA-AChE than with AChE alone. Au_{QC}@BSA-AChE is stable and they exhibit similar fluorescence on a solid substrate like filter paper, which led to the design of a highly selective, sensitive and cost effective fluorescence based optical sensor for ACh. The validity of present method tested by detecting the concentration of ACh in blood samples, which suggested its great potential for diagnostic purpose. Compared to other sensors, our sensor exhibits several practical advantages, including simple reagent preparation, sensitivity, selectivity, accuracy, cost-effective detection etc. Moreover conjugation of different enzyme on protein protected cluster can be used for development of specific sensor, which can be possible in future by following our strategy.

Acknowledgments

A.B. and T.P. thank the Department of Science and Technology, Government of India for continuous support of our research program. M.M thanks the Indian Institute of Space Science and Technology (IIST) for financial support. A.B. thanks CSIR for a fellowship

Appendix A. Supplementary material

Supplementary data associated with this article can be found in the online version at http://dx.doi.org/10.1016/j.bios.2016.02.048.

References

Baksi, A., Pradeep, T., Yoon, B., Yannouleas, C., Landman, U., 2013a. ChemPhysChem 14 (6), 1272–1282.
Baksi, A., Xavier, P.L., Chaudhari, K., Goswami, N., Pal, S.K., Pradeep, T., 2013b. Nanoscale 5 (5), 2009–2016.
Bellon, P., Manassero, M., Sansoni, M., 1972. J. Chem. Soc. Dalton Trans. 0 (14), 1481–1487.
Blokland, A., 1995. Brain Res. Rev. 21 (3), 285–300.
Chen, L.-Y., Wang, C.-W., Yuan, Z., Chang, H.-T., 2014. Anal. Chem. 87 (1), 216–229.
Chen, Z., Qian, S., Chen, X., Gao, W., Lin, Y., 2012. Analyst 137 (18), 4356–4361.
Das, T., Ghosh, P., Shanavas, M.S., Maity, A., Mondal, S., Purkayastha, P., 2012. Nanoscale 4 (19), 6018–6024.
Dass, A., 2009. J. Am. Chem. Soc. 131 (33), 11666–11667.

Feng, J.-J., Huang, H., Zhou, D.-L., Cai, L.-Y., Tu, Q.-Q., Wang, A.-J., 2013. J. Mater. Chem. C.
Ghosh, A., Jeseentharani, V., Ganayee, M.A., Hemalatha, R.G., Chaudhari, K., Vijayan, C., Pradeep, T., 2014. Anal. Chem. 86 (22), 10996–11001.
He, S.-B., Wu, G.-W., Deng, H.-H., Liu, A.-L., Lin, X.-H., Xia, X.-H., Chen, W., 2014. Biosens. Bioelectron. 62 (0), 331–336.
Heaven, M.W., Dass, A., White, P.S., Holt, K.M., Murray, R.W., 2008. J. Am. Chem. Soc. 130 (12), 3754–3755.
Hemmateenejad, B., Shakerizadeh-shirazi, F., Samari, F., 2014. Sens. Actuators B: Chem. 199, 42–46.
Huang, T., Murray, R.W., 2001. J. Phys. Chem. B 105 (50), 12498–12502.
Lakowicz, J.R., 2013. Principles of Fluorescence Spectroscopy, third Ed. Springer Science & Business Media, Germany, Chapter 8.
Le Guel̀ vel, X., Hoĭtzer, B., Jung, G., Hollemeyer, K., Trouillet, V., Schneider, M., 2011. J. Phys. Chem. C 115 (22), 10955–10963.
Li, B., Li, J., Zhao, J., 2012. J. Nanosci. Nanotechnol. 12 (12), 8879–8885.
Li, H., Guo, Y., Xiao, L., Chen, B., 2014. Analyst 139 (1), 285–289.
Li, M., Yang, D.-P., Wang, X., Lu, J., Cui, D., 2013. Nanoscale Res. Lett. 8 (1), 182.
Lin, C.-A.J., Yang, T.-Y., Lee, C.-H., Huang, S.H., Sperling, R.A., Zanella, M., Li, J.K., Shen, J.-L., Wang, H.-H., Yeh, H.-I., Parak, W.J., Chang, W.H., 2009. ACS Nano 3 (2), 395.
Liu, D., Chen, W., Tian, Y., He, S., Zheng, W., Sun, J., Wang, Z., Jiang, X., Adv. Healthcare Mater. 1 (1), 2012, 90-95.
Liu, J.-M., Cui, M.-L., Jiang, S.-L., Wang, X.-X., Lin, L.-P., Jiao, L., Zhang, L.-H., Zheng, Z.-Y., 2013. Anal. Methods 5 (16), 3942–3947.
Lystvet, S.M., Volden, S., Singh, G., Yasuda, M., Halskau, O., Glomm, W.R., 2013. RSC Adv. 3 (2), 482–495.
Mathew, A., Pradeep, T., 2014. Part. Part. Syst. Charact., n/a-n/a
Mathew, A., Sajanlal, P.R., Pradeep, T., 2012. Angew. Chem. Int. Ed. 51 (38), 9596–9600.
Mohanty, J.S., Baksi, A., Lee, H., Pradeep, T., 2015. RSC Adv. 5 (59), 48039–48045.
Mueller, S.G., Weiner, M.W., Thal, L.J., Petersen, R.C., Jack, C.R., Jagust, W., Trojanowski, J.Q., Toga, A.W., Beckett, L., 2005. J. Alzheimer's Assoc. 1 (1), 55–66.
Nair, L.V., Philips, D.S., Jayasree, R.S., Ajayaghosh, A., 2013a. Small 9 (16), 2673–2677.
Raut, S., Chib, R., Rich, R., Shumilov, D., Gryczynski, Z., Gryczynski, I., 2013a. Nanoscale 5 (8), 3441–3446.
Raut, S.L., Shumilov, D., Chib, R., Rich, R., Gryczynski, Z., Gryczynski, I., 2013b. Chem. Phys. Lett. 561–562 (0), 74–76.
Shang, L., Dong, S., Nienhaus, G.U., 2011. Nano Today 6 (4), 401–418.
Schena, A., Johnsson, K., 2014. Angew. Chem. Int. Ed. 53 (5), 1302–1305.
Soreq, H., Seidman, S., 2001. Nat. Rev. Neurosci. 2 (4), 294–302.
Watanabe, M., Kimura, A., Akasaka, K., Hayashi, S., 1986. Biochem. Med. Metab. Biol. 36 (3), 355–362.
Wei, J., Ren, J., Liu, J., Meng, X., Ren, X., Chen, Z., Tang, F., 2014. Biosens. Bioelectron. 52, 304–309.
Xavier, P.L., Chaudhari, K., Baksi, A., Pradeep, T., 2012. Nano Rev. 3, 14767.
Xie, J., Zheng, Y., Ying, J.Y., 2009. J. Am. Chem. Soc. 131 (3), 888–889.
Zhang, J., Chen, C., Xu, X., Wang, X., Yang, X., 2013. Chem. Commun. 49 (26), 2691–2693.
Zhang, L., Qv, S., Wang, Z., Cheng, J., 2003. J. Chromatogr. B 792 (2), 381–385.